Proof:

1) $R_1(L, 2N + 1) = 2[E(L - 1, N) + O(L - 1, N)]$

$$\geq 2[E(L - 1, N) + O(L - N - 1, N)]$$

$$= 2E(L, N) = 2R_2(L - 1, 2N + 1).$$

2) $R_1(L, 2N + 1) = 2[E(L - 1, N) + O(L - 1, N)]$

$$= 2[E(L - 2, N) + O(L - N - 2, N) + O(L - 1, N)]$$

$$\vdots$$

$$= 2[E(L - N, N) + \sum_{i=2}^{N} O(L - N - i, N) + O(L - 1, N)]$$

$$\geq 2[E(L - N, N) + NO(L - 2N - 1, N)] = R(L, 2N + 1).$$ □

V. Conclusion

The root structure of median roots is analyzed by applying three different appending strategies. In this correspondence, we have shown that these three appending strategies have a significant effect on the root structure and the cardinality of root set.

We also showed that the appended root signals of the median filter under the circular strategy either consist of constant neighborhoods only or consist of nonconstant neighborhoods only. It is impossible to have a median root under the circular strategy consisting of some constant neighborhoods and some nonconstant neighborhoods.

References

[1] M. Gabbouj, P.-T. Yu, and E. J. Coyle, "Convergence behavior and root signal set of stack filters," *Circuits, Syst., Signal Processing*, vol. 11, no. 1, Nov. 1992.

[2] N. C. Gallagher, Jr., and G. L. Wise, "A theoretical analysis of the properties of median filters," *IEEE Trans. Acoust., Speech, Signal Processing*, vol. ASSP-29, no. 6, Dec. 1981.

[3] P. Maragos and R. W. Schafer, "Morphological filters—Part II: Their relations to median, order statistic, and stack filters," *IEEE Trans. Acoust., Speech, Signal Processing*, vol. ASSP-35, no. 8, Aug. 1987.

[4] Z. Agur, A. S. Fraenkel, and S. T. Klen, "The number of fixed points of the majority rule," *Discrete Math.*, vol. 70, pp. 295–302, 1988.

[5] J. P. Fitch, E. J. Coyle, and N. C. Gallagher, Jr. "Median filtering by threshold decomposition," *IEEE Trans. Acoust., Speech, Signal Processing*, vol. ASSP-32, no. 6, Aug. 1984.

[6] P. D. Wendt, E. J. Coyle, and N. C. Gallagher, Jr., "Stack filters," *IEEE Trans. Acoust., Speech, Signal Processing*, vol. ASSP-34, no. 4, Aug. 1986.

[7] G. R. Arce and N. C. Gallagher, Jr., "State description for the root-signal set of median filters," *IEEE Trans. Acoust., Speech, Signal Processing*, vol. ASSP-30, no. 6, Dec. 1982.

[8] J. P. Fitch, E. J. Coyle, and N. C. Gallagher, Jr., "Root properties and convergence rates of median filters," *IEEE Trans. Acoust., Speech, Signal Processing*, vol. ASSP-33, no. 1, Feb. 1985.

[9] D. Eberly, H. Longbotham, and Jorge Aragon, "Complete classification of roots to one-dimensional median and rank-order filters," *IEEE Trans. Acoust., Speech, Signal Processing*, vol. 39, no. 1, Jan. 1991.

[10] C. L. Liu, *Elements of Discrete Mathematics*, 2nd ed. New York: McGraw-Hill, 1985.

On Stability of Reconstruction from Fourier Transform Modulus

Avideh Zakhor

***Abstract*—We derive the lower bound on the condition number of reconstruction of two classes of sequences from their Fourier transform magnitude (FTM). The lower bound for one class is shown to be 1, and for another class to be $1/2N^{Q/2}$, where Q is the dimensionality of the sequence and N is the number of nonzero elements in each dimension. Stability of reconstruction from FTM and space domain phase is discussed. It is found that randomizing the space domain phase improves reconstruction robustness. Experimental results are presented to verify theoretical predictions.**

I. Introduction

Multidimensional (M-D) signal reconstruction from Fourier transform magnitude (FTM) has been an active area of research for a number of years [1]–[8]. Although uniqueness of reconstruction has been shown from a theoretical point of view [5], there seems to be no practical, stable algorithms resulting in satisfactory reconstruction of a broad class of signals. Specifically, iterative algorithms suffer from stagnation [7], [8], and closed form solutions seem to work well only with small images [9].

In this correspondence, we consider the stability of the problem of reconstruction from FTM. Specifically, we derive conditions under which various classes of M-D signals can be reconstructed in a stable or unstable fashion. Our stability results are algorithm independent in the sense that we are primarily concerned with problem stability rather than algorithm stability. The outline of the remainder part of this correspondence is as follows. Section II briefly reviews the concept of condition number of a problem and its algorithms from a numerical analysis point of view. Section III includes this correspondence's main result on conditions of stability, and Section IV states the conclusions.

II. Problem and Algorithm Stability

A problem S, can be defined as a mapping, possibly nonlinear, from data $\vec{x}$ to solution $\vec{y}$, denoted by $S: \vec{x} \rightarrow \vec{y} = S(\vec{x})$. A simple example of a problem is finding the square root of a real number. A problem is said to be well conditioned if small relative changes in data lead to small relative changes in the solution. A measure of stability of the problem S at point $\vec{x}$ is its condition number which is defined to be [10]

$$K(S; \vec{x}) = \lim_{\epsilon \rightarrow 0} \sup_{\|\Delta x\| = \epsilon} \frac{\|S(\vec{x} + \Delta\vec{x})\| / \|S(\vec{x})\|}{\|\Delta\vec{x}\| / \|\vec{x}\|}.$$

The above expression is essentially the ratio between relative change in solution and relative change in data. A problem is said to be well conditioned at point $\vec{x}$, if its condition number is small, i.e., of the order of 1. Likewise, it is said to be ill conditioned if

Manuscript received May 9, 1991; revised February 24, 1992. This work was supported by grants from the following organizations: NSF-PYI Grant MIP-9057466, Joint Services Electronics Project, and ONR Young Investigator Award N00014-92-J-1732. This work was presented in part at the 1990 International Conference on Acoustics, Speech, and Signal Processing, Albuquerque, NM.

The author is with the Department of Electrical Engineering and Computer Sciences, University of California, Berkeley, CA 94720.

IEEE Log Number 9205128.

1053-587X/93$03.00 © 1993 IEEE

its condition number is large, e.g., greater than 10^2. An example of a well-conditioned problem is taking the square root at a point $x \in [0, \infty]$, whose condition number is given by

$$K(S, x) = \lim_{\epsilon \to 0} \sup_{\|\Delta x\| = \epsilon} \frac{|\sqrt{x + \delta x} - \sqrt{x}| / |\sqrt{x}|}{|\delta x| / |x|}.$$

Approximating $\sqrt{x + \delta x} \approx \sqrt{x} + d/dx(\sqrt{x})\, \delta x$, the above condition number can be shown to be $1/2$. An example of a problem which can be ill conditioned at some data points is that of finding roots of a polynomial, specially if has multiple roots. For example, the polynomial $x^2 - 2x + 1$ has double roots at 1. However, if its last coefficient is perturbed by 10^{-4} to $x^2 - 2x + 0.9999$, then its roots move by 10^{-2} to 0.99 and 1.01. Thus, the condition number of finding the roots of the above polynomial is lower bounded by $10^{-2}/10^{-4} = 100$.

The notion of stability of an algorithm is quite distinct from that of a problem. An algorithm is said to be stable at a specific data point if the sensitivity of its numerical answer to the data is no greater than that of the original mathematical problem. A well-conditioned problem might have stable or unstable algorithms. For instance, solving a linear system of equations could be unstable if Gaussian elimination without pivoting is used, even though pivoting can greatly improve its stability. Similarly, determining the smallest root x_2 of the quadratic polynomial $x^2 + 2bx + c$ with $b < 0$ and c given to t digits with $|c|/b^2 < 10^{-t}$ is unstable if x_2 is computed via

$$x_2 = -b - \sqrt{b^2 - c}.$$

On the other hand, if the larger root x_1 is computed by $x_1 = -b + \sqrt{b^2 - c}$, and the smaller root is computed via $x_2 = c/x_1$, then x_2 can be shown to be determined in a stable fashion [11]. While a well-conditioned problem might have a stable or unstable algorithm, an ill-conditioned problem cannot have a stable algorithm. For instance, solving linear least squares problems for an ill-conditioned matrix is ill conditioned, regardless of the algorithm applied to it.

In the remainder of this correspondence, we address the stability of the problem of reconstruction from FTM. Our approach is different from some of the statistical approaches in the literature in which estimation theory is used to derive a Cramer–Rao bound on the mean-squared error of the estimate of the object from measurements of the intensity of its Fourier transform [15]. Instead, we derive lower bounds on the condition number of the reconstruction problem for various signal classes.

III. Stability of Reconstruction from FTM

In this section, we analyze stability properties of the problem of reconstruction from FTM. Specifically, we will show that the lower bound on the condition number of the reconstruction problem is highly signal dependent. To avoid notational complexity, we primarily deal with stability issues of the one dimensional (1-D) case, even though the solution in 1-D has been shown not to be unique. The analysis can be extended to two and higher dimensions in a straightforward fashion.

Consider an N point, real, positive, one-dimensional sequence $x(n)$ with its Fourier transform denoted by $X(\omega)$. If P is an integer greater than one, and $\vec{M}$ denotes the PN-dimensional vector consisting of PN equispaced samples of $|X(\omega)|^2$, then the problem of reconstruction from samples of FTM can be considered as a nonlinear map between a PN-dimensional data vector $\vec{M}$ and a N-dimensional solution vector $\vec{x}$, i.e., $S: \vec{M} \to \vec{x}$ where solution vector $\vec{x}$ consists of the elements of the sequence $x(n)$. Our goal can then be stated as finding the condition number of the above problem for different classes of sequences. To accomplish this, we perturb the data by $\delta\vec{M}$, find the perturbation to the solution $\delta\vec{x}$, and form the ratio:

$$\frac{\|\delta\vec{x}\| / \|\vec{x}\|}{\|\delta\vec{M}\| / \|\vec{M}\|}. \tag{1}$$

Clearly, perturbations of $\vec{M}$ along different directions result in different values for the above expression. Condition number of the problem however, is the particular perturbation $\delta\vec{M}^*$ which maximizes the above ratio. Finding this perturbation involves constrained nonlinear optimization, and in general is not an easy task. Our approach, however, is to find a lower bound for the condition number by finding one particular perturbation.

Consider the perturbation sequence

$$\delta x(n) = \begin{cases} \epsilon & n = 0 \\ 0 & n \neq 0 \end{cases} \tag{2}$$

and its corresponding perturbed sequence $x'(n) \equiv x(n) + \delta x(n)$. If $X'(\omega)$ denotes the Fourier transform of $x'(n)$, and $\vec{M}'$ denotes the perturbed FTM vector whose elements are uniformly spaced samples of $|X'(\omega)|^2$, then the resulting perturbation in FTM is given by $\delta\vec{M} \equiv \vec{M}' - \vec{M}$. We now use the perturbation of (2) to derive a lower bound for different classes of sequences.

A. Spatially Extended Sequences

We begin with the following theorem.

Theorem 1: Consider a positive, real N point sequence $x(n)$ which satisfies the following condition:

$$\frac{\sum_{k=0}^{PN-1} \left(\sum_{n=0}^{N-1} x(n) \cos\left(\frac{2\pi kn}{PN}\right)\right)^2}{\sum_{k=0}^{PN-1} M_k^2} \approx \frac{\left[\sum_{n=0}^{N-1} x(n)\right]^2}{M_0^2} \tag{3}$$

where M_0 stands for the DC component of the FTM vector $\vec{M}$. The approximate lower bound for the condition number of the problem of reconstruction from PN samples of FTM of the one-dimensional sequence $x(n)$ is:

$$K(S; \vec{x}) > \frac{\sum_{n=0}^{N=1} x(n)}{2\sqrt{\sum_{n=0}^{N-1} x^2(n)}}. \tag{4}$$

The approximate lower bound for the condition number of reconstruction of a Q-dimensional sequence from $PN \times PN \times \cdots \times PN$ samples of FTM is given by

$$K_Q(S; \vec{x}) > \frac{\sum_{n_1=0}^{N-1} \sum_{n_2=0}^{N-1} \cdots \sum_{n_Q=0}^{N-1} x(n_1, n_2, \cdots, n_Q)}{2\sqrt{\sum_{n_1=0}^{N-1} \sum_{n_2=0}^{N-1} \cdots \sum_{n_Q=0}^{N-1} x^2(n_1, n_2, \cdots, n_Q)}}. \tag{5}$$

Furthermore, if the first and second moment of $x(n)$ can be approximated in the following way:

$$\langle x(n) \rangle_n \equiv \frac{1}{N} \sum_{n=0}^{N-1} x(n) \approx A \tag{6}$$

$$\langle x^2(n) \rangle_n \equiv \frac{1}{N} \sum_{n=0}^{N-1} x^2(n) \approx A^2 \tag{7}$$

TABLE I
PREDICTED AND ACTUAL VALUES FOR THE LOWER BOUND ON THE CONDITION NUMBER

Image	Size $N \times N$	Approx. Th. $N/2$	Experiment Equation (1)	Approx. Th. Inequality (5)
Cameraman	32 × 32	16	13.6	14.9
Cameraman	64 × 64	32	27.2	29.8
Cameraman	128 × 128	64	54.3	59.7
Cameraman	256 × 256	128	108.6	119
Vegas	32 × 32	16	12.0	13.5
Vegas	64 × 64	32	24.1	26.9
Vegas	128 × 128	64	48.3	53.9
Vegas	256 × 256	128	106.2	114.9
Boat	32 × 32	16	12.36	14.05
Boat	64 × 64	32	24.8	28.2
Boat	128 × 128	64	49.7	56.5
Boat	256 × 256	128	99.5	113.3
Brow	32 × 32	16	11.9	14.4
Brow	64 × 64	32	23.8	28.8
Brow	128 × 128	64	48.2	58
Cameraman with delta	32 × 32	N/A	0.5	0.8

then the approximate lower bounds for one, two, and Q dimensional sequences grow as $\sqrt{N}/2$, $N/2$, and $N^{Q/2}/2$, respectively.

Proof: Consider the perturbation shown in (2). For small values of ϵ, we can approximate the kth element of the FTM perturbation vector in the following way:

$$\delta M_k \approx 2\epsilon \sum_{n=0}^{N-1} x(n) \cos\left(\frac{2\pi kn}{PN}\right). \tag{8}$$

Combining the above equation with (3), we conclude that

$$\frac{\|\delta\vec{M}\|_2}{\|\vec{M}\|_2} \approx 2\epsilon \frac{\sum_{n=0}^{N=1} x(n)}{\left(\sum_{n=0}^{N-1} x(n)\right)^2}.$$

Using above equation and taking into account that

$$\|\vec{x}\|_2 = \sqrt{\sum_{n=1}^{N-1} x^2(n)}$$

the lower bound on the condition number of the reconstruction problem can be written as

$$K(S;\vec{x}) > \frac{\sum_{n=0}^{N-1} x(n)}{2\sqrt{\sum_{n=0}^{N-1} x^2(n)}}. \tag{9}$$

Using the approximate moment assumptions of (6) and (7), the approximate lower bound becomes

$$E[K(S,\vec{x})] > \frac{\sqrt{N}}{2}. \tag{10}$$

We can extend this argument to higher dimensions and conclude that the expected value of the condition number of two-dimensional and Q-dimensional signals is lower bounded by $N/2$ and $N^{Q/2}/2$, respectively. □

The above theorem provides an approximate rather than an exact lower bound on the condition number of FTM reconstruction problem. This is because conditions (3), (6), and (7) only impose approximate rather than exact reconstructions on the signals under consideration. Indeed if the approximate signs in assumptions (3), (6), and (7) are replaced by equalities, the approximate lower bound provided by Theorem 1 also becomes exact.

We now investigate a subclass of signals that satisfy conditions of the above theorem. Since we are primarily interested in FTM reconstruction for images, we restrict our discussion to two-dimensional signals. The assumption associated with (3) can be justified by noting that for a broad class of signals, the numerator (denominator) of the left side of (3) can be approximated with the numerator (denominator) of the right side of the equation. Specifically, the denominator approximation requires the norm of the FTM vector of the signal under consideration to be dominated by its DC component, and the numerator approximation requires the norm of the FTM vector of the even part of the signal under consideration to be dominated by its DC component. Therefore, roughly speaking, assumption (3) holds, among other classes of images, for a class of images in which most of the energy in the Fourier domain is concentrated around DC, or more generally low frequency terms. We refer to this class of signals as "DC dominant."

Our second comment has to do with assumptions (6) and (7). Specifically, if the first moment of the sequence $x(n)$ is exactly equal to A, then its second moment is greater than or equal to A^2, with equality if and only if $x(n) = A$ for all $1 \le n \le N$. Thus, strictly speaking, assumptions (6) and (7) can only be exactly true for the class of constant signals, and therefore the bound shown in (10) is only exactly true for constant signals. However, the bound in (10) is approximately true for sequences which approximately satisfy (6) and (7), that is for sequences whose elements are more or less uniformly distributed. We refer to these sequences as "extended" rather than "peaky" images in which the majority of pixels have small (large) intensity values and only a few are bright (dark). In fact, the more uniformly distributed a signal looks in the space domain, the more accurately it satisfies assumptions (6) and (7).

Note that DC dominant signals are not the only ones satisfying (3). In fact, a peaky signal of the form $x(0) = 1$ and $x(n) = 0$ for all $n \neq 0$ also satisfies (3), even though the denominator (numerator) of the left-hand and right-hand sides of (3) are not approximately equal to the denominator (numerator) of the right hand side.

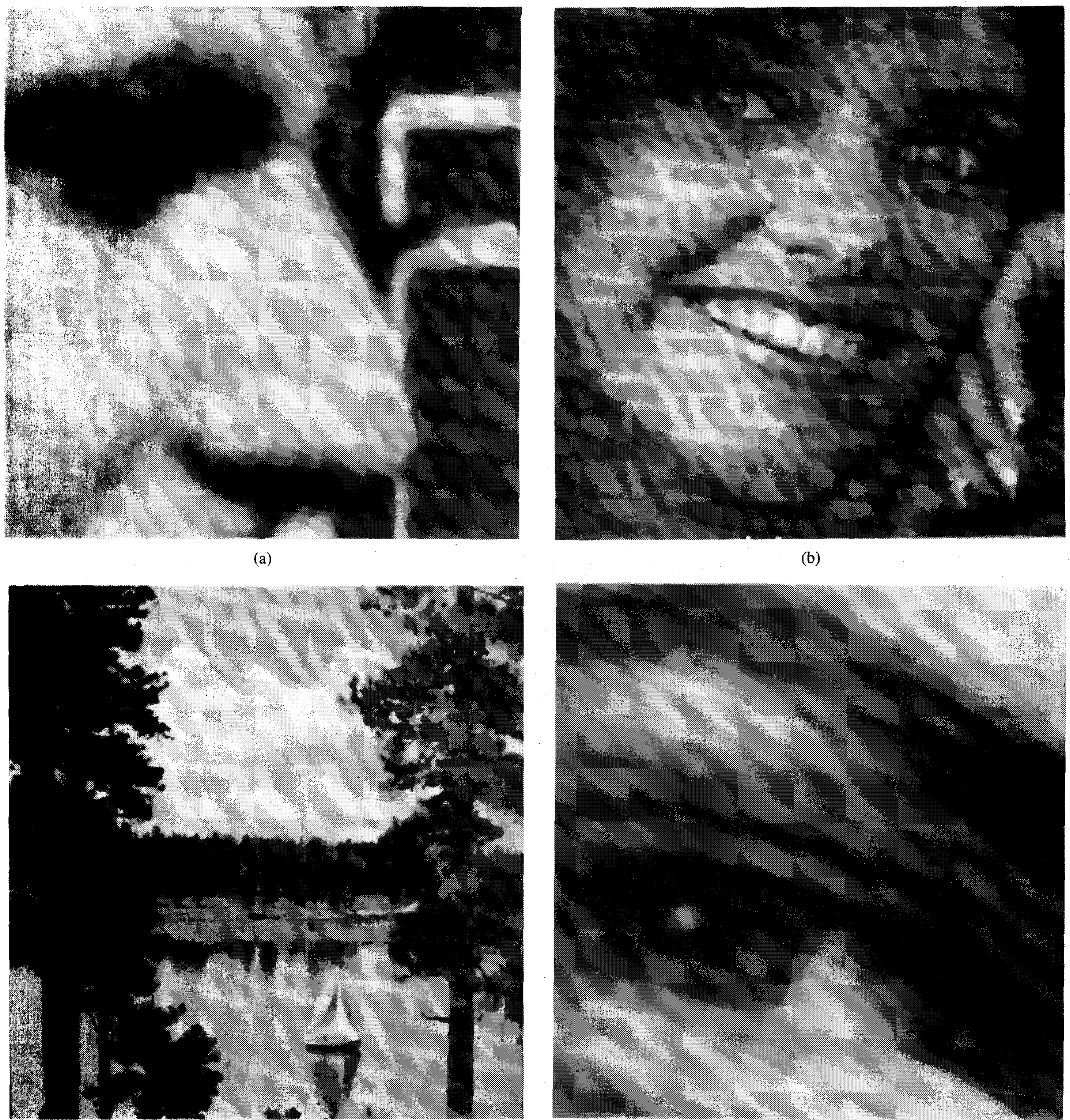

(a) (b) (c) (d)

Fig. 1. Original (a) 256 × 256 cameraman; (b) 256 × 256 vegas; (c) 256 × 256 boat; (d) 128 × 128 brow.

Thus, the lower bound of (5) applies to this signal. However, since the signal does not satisfy the moment assumptions of Theorem 1, the $\sqrt{N}/2$ lower bound of (10) does not apply to it. We will comment on this issue again at the end of Section III-A.

Table I shows the predicted and actual values of the lower bound on the condition number of the reconstruction problem for the "cameraman," "vegas," "boat," and "brow" images whose originals are shown in Fig. 1. All the pictures are 256 × 256 except for the "brow" which is 128 × 128. Each set of images in Table I consists of four different resolutions ranging from 32 × 32 to 256 × 256. Subsampling is used to obtain lower resolution images from higher resolution ones. The third column of the table shows the approximate theoretical lower bound of Theorem 1, i.e., $N/2$ for two-dimensional images of size $N \times N$. The fourth column of the table shows the experimental lower bounds obtained by using the perturbation sequence shown in (2), computing the perturbation in FTM vector norm, and forming the ratio shown in (1). The experimental results are robust with respect to the value of ϵ in (2). The particular value we chose for Table I is $\epsilon = 0.01$. As seen, the experimental lower bound of the fourth column is in excellent agreement with the approximate theoretical bounds in the third column, indicating that the images under considerations satisfy the assumptions of Theorem 1. Furthermore, as expected, the theoretical and experimental lower bounds on condition numbers double as the size of the images under consideration doubles.

The last column of Table I shows the right-hand side of inequality (5), which is solely based on assumption (3) and therefore does not require the validity of the moment assumptions shown in (6) and (7). As seen, the values in the last column are very close to the experimental lower bound, indicating the validity of assumption (3) for the images considered in the table. Finally, for each row in Table I, the entries of the experimental column is closer to those of the last column than to the entries of the third column. This can be attributed to the fact that the entries on the last column only require assumption (3), while those of the third column require additional assumptions (6) and (7).

The last row of Table I shows the properties of a "peaky" signal obtained by adding a delta function of a large amplitude to location (0, 0) of the 32 × 32 cameraman signal in the first row of the table. The amplitude of the delta function is 3×10^5, while the remaining elements of the sequence are between 0 and 255. Since this results in a peaky signal, it does not satisfy the moment assumptions of Theorem 1, and hence $N/2$ is not a valid lower bound for it. Furthermore, neither the norm of its FTM vector nor the FTM vector of its even part are dominated by its DC component, and hence it is not a "DC dominated" signal. Specifically, in the assumption of (3) in Theorem 1, the denominator of the left-hand side is 650 times larger than the denominator of the right-hand side, and the numerator of the left-hand side is 1600 times larger than the numerator of the right-hand side.[1] Nevertheless, assumption (3) is approximately (within a factor of 2.5) satisfied for this signal and hence the bound in (5) is a valid lower bound for its condition number. This bound is shown in the last column of Table I to be 0.8. The experimental lower bound obtained via (1) is shown in the fourth column of Table I to be 0.5. Thus, the experimental lower bound is quite close to the theoretical one in (5). In Theorem 2 of the next section, we find another lower bound for this signal, which unlike (5) is independent of the elements of the signal itself.

A. Frequency Extended Sequences

In the previous section, we derived a lower bound on the condition number of signals for which the norm of the FTM vector of a signal $\|\vec{M}\|_2$ and its even component $\|\delta\vec{M}\|_2$ are dominated by their DC component. In this section, we are interested in signals for which the elements of the FTM vector contribute more or less uniformly to its norm. We can show the following theorem.

Theorem 2: Consider a real or completed valued N point sequence $x(n)$ with FTM vector $\vec{M}$ satisfying the following moment properties:

$$\langle M_k \rangle_k \equiv \frac{1}{PN} \sum_{k=0}^{PN-1} M_k \approx A^2 \tag{11}$$

$$\langle M_k^2 \rangle_k \equiv \frac{1}{PN} \sum_{k=0}^{PN-1} M_k^2 \approx A^4 \tag{12}$$

$$\left\langle \left| \sum_{n=0}^{N-1} x(n) \cos\left(\frac{2\pi kn}{PN}\right) \right|^2 \right\rangle_k \approx \frac{A^2}{2}. \tag{13}$$

The lower bound for the condition number of the problem of reconstruction from PN samples of the FTM of $x(n)$ is 1. For two-dimensional $N \times N$ sequences, or more generally, Q-dimensional signals, the lower bound is also 1.

Proof: The assumption of (12) implies that

$$\|\vec{M}\|_2 \approx A^2\sqrt{PN}.$$

If the particular perturbation we consider is the one shown in (2), then the assumption shown in (13) together with (8) imply

$$\|\delta\vec{M}\|_2 \approx \epsilon A\sqrt{PN}.$$

Using Parseval's relation together with (11) we get

$$\|\vec{x}\| \approx A.$$

Combining the above three equations, and taking into account that $\|\delta\vec{x}\|_2 \approx \epsilon$, we conclude that

$$K(S; \vec{x}) > 1.$$

The derivation for two and higher dimensions is identical. □

Note that satisfying Theorem 2's conditions does not guarantee that the reconstruction problem is well conditioned. Rather, it implies that the lower bound on the condition number of the problem is one, and therefore there is some hope for stable reconstruction. After all, even if the lower bound on the condition number is one, the actual condition number could be very large and the problem could still be quite ill conditioned. Therefore, only when the lower bound on the condition number is very large, as in Theorem 1, can we claim ill conditionedness of the problem. However, if the lower bound is low, the problem could be either well or ill conditioned.

Theorem 2 is dual of Theorem 1 in a sense that conditions shown in (6) and (7) of Theorem 1 are space domain counterparts of the frequency domain conditions of (11) and (12) of Theorem 2. Roughly speaking, signals for which the distribution of the elements of the FTM vector is more or less uniform can be shown to satisfy conditions (11) and (12) of Theorem 2. This is in sharp contrast with signals associated with Theorem 1 in which the main contribution to the norm of the magnitude vector is from a few elements only.

A subclass of signals satisfying (11) and (12) of Theorem 2 is "peaky" images. An application in which peaky images occur frequently is optical astronomy. Examples of successful reconstruction from FTM for such images have been reported in the literature [1]. Another way to obtain peaky images would be to add the function $A\delta(n_1 - m_1, n_2 - m_2)$ to a spatially extended sequence whose elements are considerably smaller than A. For instance, we have found that adding a large amplitude impulse to the (0, 0)th element of the cameraman picture shown in Fig. 2(a) flattens the FTM and results in successful recovery from FTM. As will be shown later, without adding this delta function, complete recovery of cameraman from it FTM is not possible.[2]

A similar application in which the FTM is deliberately flattened is acoustical, microwave, or optical Fourier transform holography with a reference wave [12]. This involves adding a reference wave such as a plane wave e^{jbx} to the light wave $g(x, y)$ due to the Fourier transform of the object $p(u, v)$, squaring the absolute value of the sum to get $h(x, y)$, and producing a film transparency with an amplitude transmittance proportional to $h(x, y)$, which is positive and real. Optical and numerical reconstruction of the object $p(u, v)$ have been successfully demonstrated [12].

Another well-known technique in optical holography to flatten FTM is to multiply each pixel of a two-dimensional signal by a

[1]For comparison purposes, for the 32 × 32 cameraman without the delta function, the denominator (numerator) of the left-hand side of (3) is twice the denominator (numerator) of its right-hand side.

[2]Once again, we are not claiming that flattening FTM improves the condition number of the problem. All we are stating is that the lower bound on the condition number becomes small as FTM as flattened.

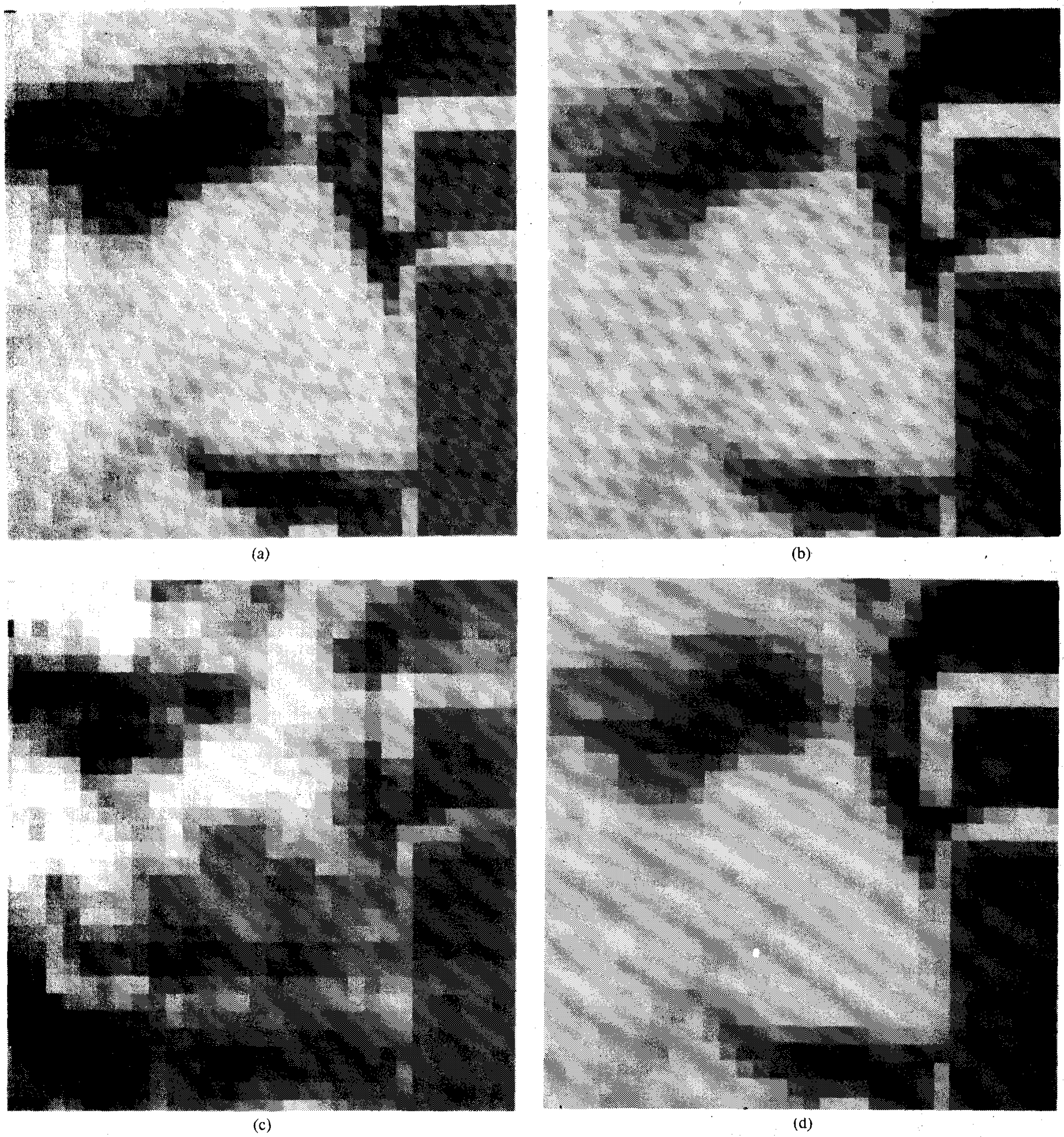

Fig. 2. (a) Original 32 × 32 cameraman; (b) reconstruction from FTM and known random phase; (c) reconstruction from FTM only; (d) reconstruction from and one bit of space.

random phase factor before computing its Fourier transform. In the absence of the random phase, the magnitude of the DC and low frequency components become much larger than those of higher frequencies, thus posing a severe problem in recording the Fourier transform on film [12]. Another application in which random phase improves the robustness of a reconstruction problem is in [14] where it is shown that the band-limited extrapolation problem in the frequency domain is considerably more robust when the signal under consideration has random space domain phase.

Theorem 2 can be used to explain the stability of FTM reconstruction of spatially extended signals with known random space domain phase. While the FTM of spatially extended signals, such as the cameraman, satisfy the conditions of Theorem 1, the FTM of their corresponding signal resulting from random phase assignment satisfies the conditions of Theorem 2. Thus, the addition of random phase in space domain improves the lower bound on the condition number of the problem of FTM reconstruction. For instance, the computed lower bounds on the condition number of the

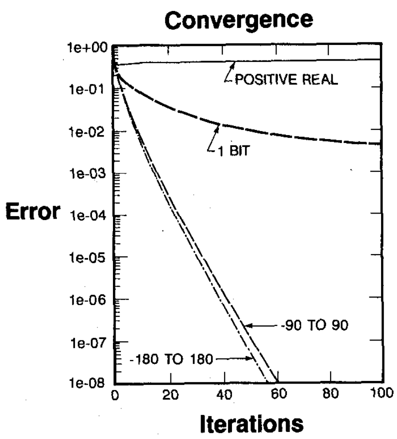

Fig. 3. Reconstruction error as a function of iteration number for reconstruction from FTM alone, FTM with one bit of phase, and FTM with known random phase.

problem of reconstruction of the 32 × 32 and 64 × 64 cameraman, and 32 × 32 brow image from the FTM of their corresponding sequences, after random phase has been added to each pixel, are 0.09986, 1.0091, and 1.0011, respectively. These numbers are obtained by using the perturbation sequence shown in (2) and forming the ratio shown in (1). The corresponding lower bounds without the random phase component are shown in the third column of Table I, and are 13.6, 27.2 and 11.9, respectively.

The small lower bound on condition number in the case of known random phase images directly translates into practical reconstruction of these sequences using iterative algorithms such as the Gerchberg–Saxton [4]. Specifically, an example of the reconstruction of 32 × 32 cameraman shown in Fig. 2(a), from the 64 × 64 samples of the FTM of its corresponding sequence after a known random phase has been added to each pixel, is shown in Fig. 2(b). The known random phase for each pixel is uniformly distributed in $(0, 2\pi)$. As seen, the quality of reconstruction is indistinguishable from the original. For comparison purposes, the reconstruction from 64 × 64 samples of FTM, without the random phase is also shown in Fig. 2(c).

From the above example, it is seen that reconstruction of the cameraman image is ill conditioned if the known phase associated with all the pixels in the space domain is zero, and well conditioned if the known phase associated with each pixel is uniformly distributed between 0 and 2π. A special intermediate case between the above two extremes is when the space domain phase takes on signal dependent, binary values of 0 or π. For instance, if the pixels above and below a certain known threshold are associated with phases 0 and π, respectively, then the problem of reconstruction from known random phase and FTM becomes equivalent to reconstruction from FTM and one bit of space domain information. Fig. 2(d) shows the reconstruction of the original 32 × 32 cameraman shown in Fig. 2(a), from 64 × 64 samples of its FTM and one bit of the space domain, obtained by thresholding Fig. 2(a). As seen, the quality of reconstruction in Fig. 2(d) is considerably higher than that of reconstruction from FTM alone shown in Fig. 2(c).

Finally, to quantify the reconstruction quality shown in Fig. 2, we present results on convergence of the iterative Gerchberg–Saxton algorithm for reconstruction from FTM and known space domain phase. Fig. 3 shows the mean squared error (MSE) between the actual and reconstructed image as a function of iteration number. The magnitude of the space domain signal used for reconstruction, corresponds to the positive, real intensities of the pixels of the 32 × 32 cameraman shown in Fig. 2(a), while the phase for each pixel is a uniformly distributed random variable in the range $(-\theta, +\theta)$. Different curves in Fig. 3 correspond to various values of θ. Clearly, an increase in the variance of the space domain phase results in a decrease in MSE and faster convergence. Furthermore, the speed of convergence for reconstruction from one bit of space is in between that of zero phase, and randomly distributed phase in $(0, 2\pi)$.

IV. Summary and Conclusions

We derived the lower bound on the condition number of the problem of reconstruction for two classes of signals. The lower bound for spatially extended $N \times N$ images in which the norm of the FTM vector is dominated by DC and low frequency components, was shown to grow with N. The lower bound for images in which the low and high frequency elements of the FTM vector contribute more or less equally to its norm, is 1.

We discussed the problem of reconstruction from FTM and known phase in space domain. Since the introduction of sufficiently random space domain phase results in "flattened" FTM distribution, the lower bound on the condition number of the reconstruction problem with respect to the FTM vector again becomes one. This is in agreement with our experimental results indicating that randomizing the phase in space domain improves the convergence rate of the Gerchberg–Saxton algorithm.

We end this correspondence with a note of caution on the interpretation of the presented results. It is important to emphasize that all the results in here dealt with *lower bounds* on condition numbers rather than the actual condition number. This implies that, even though Theorem 2 indicates lower bound of 1 for certain classes of sequences, the reconstruction problem is not necessarily well posed for all the sequences in these classes. For example, it is well known that the region of support of the sequences under consideration is of importance in reconstruction of two-dimensional sequences [1]. Therefore, all that we can claim here is that there is some hope for successful recovery under certain conditions.

Acknowledgment

The author gratefully acknowledges K. Shirriff's assistance in generating the curves in Fig. 3.

References

[1] R. H. T. Bates and M. J. McDonnell, *Image Restoration and Reconstruction.* Oxford: Clarendon; New York: Oxford University Press, 1986.
[2] N. E. Hurt, *Phase Retrieval and Zero Crossings.* Netherlands: Kluwer Academic.
[3] T. T. Huang, J. L. C. Sanz,and W. Blanz, "Image representation by one-bit Fourier phase: Theory, sampling, and coherent image model," *IEEE Trans. Acoust., Speech, Signal Processing*, vol. 36, no. 8, pp. 1292–1304, Aug. 1988.
[4] F. R. Fienup, "Phase retrieval algorithms: A comparison," *Appl. Opt.*, vol. 21, no. 15, pp. 2758–2769, Aug. 1982.
[5] M. H. Hayes, "The reconstruction of a multidimensional sequence from the phase or magnitude of the Fourier transform," *IEEE Trans. Acoust., Speech, Signal Processing*, vol. ASSP-30, pp. 140–154, 1982.
[6] J. L. C. Sanz, T. S. Huang, and F. Cukierman, "Stability of unique Fourier transform phase reconstruction," *J. Opt. Soc. Amer.*, vol. 73, pp. 1442–1445, 1983.
[7] J. R. Fienup, "Reconstruction of a complex valued object form the modulus of its Fourier transform using a support constraint," *J. Opt. Soc. Amer.*, vol. 4, no. 1, pp. 119–123, Jan. 1987.
[8] H. Stark, *Image Recovery: Theory and Applications.* New York: Academic, 1987.
[9] J. S. Lim and D. Izraelevitz, "A new direct algorithm for image reconstruction from Fourier transform magnitude," *IEEE Trans. Acoust., Speech, Signal Processing*, pp. 511–519, Apr. 1987.

[10] G. H. Golub, *Studies in Numerical Analysis.* Mathematical Association of America, 1984.
[11] E. Isaacson and H. B. Keller, *Analysis of Numerical Methods.* New York: Wiley, 1966.
[12] T. S. Huang, "Digital holography," *Proc. IEEE*, vol. 59, no. 9, pp. 1335–1346, Sept. 1971.
[13] F. R. Fienup and C. C. Wackerman, "Phase-retrieval stagnation problems and solutions," *J. Opt. Soc. Amer.*, vol. 3, no. 11, pp. 1987–1907, Nov. 1986.
[14] D. C. Munson and J. L. C. Sanz, "Image reconstruction from frequency-offset Fourier data," *Proc. IEEE*, vol. 72, no. 26, pp. 661–669, June 1984.
[15] J.N. Cederquist and C. C. Wackerman, "Phase retrieval error: A lower bound, *J. Opt. Soc. Amer.*, vol. 4, no. 9, pp. 1788–1792, Sept. 1987.

Direct Frequency-Domain Deconvolution when the Signals Have No Spectral Inverse

Damjan Zazula and Ludvik Gyergyek

***Abstract*—We describe a new method of frequency-domain deconvolution when the kernel has no spectral inverse. Discrete frequency interpolation is used to avoid zero-valued frequency samples. The algorithm does not suffer from the spectral singularities of the original kernel, its complexity is proportional to the fast Fourier transform, and a comparative noise study showed improved performance relative to the direct frequency-domain method.**

I. Introduction

When we are interested in the characteristics of a system, it is very natural to observe the system operation referring to its output signal. Then, the characteristic behavior is generally explained either by the impulse response in an input–output model or by the internal state changes in a state-space model. Nevertheless, to establish the backward connection from the system output to its characteristics or input signals, we face the inverse problem that is to be solved by a kind of deconvolution.

Many different approaches to deconvolution have been introduced. Some of them attempt to avoid instability of frequency-domain deconvolution; some, however, obtain the deconvolution result given the system output signal, but not its impulse response nor the input signal. The former acquires the answer in time-domain algorithms using smoothing filters [1] or interative gradient methods [2]. The latter is important especially when dealing with hardly controllable systems, e.g., in observing natural and biomedical phenomena [3]. Another approach, used mainly in speech and seismic signal processing, is homomorphic deconvolution [4].

All these approaches are computationally more complex than simple direct deconvolution in the frequency domain, realized by the fast Fourier transform (FFT). Unfortunately, frequency-domain deconvolution is not feasible when the kernel has no spectral inverse. Some successful, though computationally very complex algorithms (proportional to N^4) have been developed in the time domain [5].

Manuscript received February 2, 1990; revised January 13, 1992.

D. Zazula is with the Faculty of Technical Sciences Maribor, Department of Computer Science, 62000 Maribor, Slovenia.

L. Gyergyek is with the Faculty of Electrical Engineering and Computer Science in Ljubljana, Department of Systems and Control Engineering, 61000 Ljubljana, Slovenia.

IEEE Log Number 9205121.

In this correspondence, we define a frequency-domain method using interpolated frequency samples that does not suffer from the spectral singularities. We present a computer algorithm based on the FFT to implement the method, and we study the influence of noise added to the signals.

II. Discrete Fourier Transform of Real Sampled Signals

In all discrete signal processing applications where the processed signal period must be relatively long with respect to the sampling interval, the number of samples is rather high. The z transform of the sampled signal is a high-degree polynomial in z which has integer coefficients, with the maximum value restricted to the range of quantization levels of the A/D converter used. Such polynomials can have roots only in certain regions of the z plane [6], so the distribution of zeros on the unit circle is not arbitrary. Consider a polynomial $p(z)$ in z of order N with random coefficients. Let $M(\varphi_1, \varphi_2)$ be the number of zeros of $p(z)$ having angles between φ_1 and φ_2. It is shown in [7] that, with probability 1,

$$\lim_{N \to \infty} \frac{M(\varphi_1, \varphi_2)}{N} = \frac{\varphi_2 - \varphi_1}{2\pi}; \qquad 0 \le \varphi_1 \le \varphi_2 \le 2\pi.$$

This result indicates that, as N becomes large, the zeros of $p(z)$ tend to become evenly distributed in angle. Thus the spacing of the zeros tends to $2\pi/N$, which is the spacing of the frequency samples computed by an N-point DFT. If one then samples $p(z)$ with a DFT of length $2N$ (interpolation), it is unlikely that adjacent even- and odd-numbered Fourier coefficients will equal 0 at the same time because their angular spacing is π/N, while the zeros tend to be $2\pi/N$ apart.

III. An Algorithm for Frequency-Domain Deconvolution

The previous discussion suggests that if a signal's N-point DFT has zeros, then interpolated spectral samples would differ from zero. Therefore, using the sequence of the interpolated samples as a deconvolution kernel, the singularities would be eliminated.

Consider an arbitrary discrete system with unit-sample response $h(n)$ and output signal $y(n)$, $n = 0, \cdots, N-1$. Denote their DFT's $H(k)$ and $Y(k)$, $k = 0, \cdots, N-1$. Let the sequences $H_1(k)$ and $Y_1(k)$, $k = 0, \cdots, 2N-1$, be the $2N$-point DFT's of the $2N$-point signals $h_1(n)$ and $y_1(n)$, $n = 0, \cdots, 2N = 1$, where

$$h_1(n) = \begin{cases} h(n); & n = 0, \cdots, N-1 \\ 0 & n = N, \cdots, 2N-1 \end{cases}$$

$$y_1(n) = \begin{cases} y(n); & n = 0, \cdots, N-1 \\ 0 & n = N, \cdots, 2N-1 \end{cases}$$

Next, note that

$$\begin{aligned} H_1(2l+1) &= \sum_{n=0}^{N-1} h_1(n) \cdot W_{2N}^{n(2l+1)} \\ &= \sum_{n=0}^{N-1} h(n) \cdot W_{2N}^{n} \cdot W_N^{nl} \\ &= \text{DFT}\,[h(n) \cdot e^{-j(\pi/N)n}] \end{aligned} \tag{3.1}$$